MPPT based sliding mode control for fuel cell connected grid system

El Otmani, F.; Abouloifa, A.; Aourir, M.; Lachkar, I.; Assad, F. Z.; Giri, F.; Guerrero, J. M.

Published in:
IFAC-PapersOnLine

DOI (link to publication from Publisher):
10.1016/j.ifacol.2020.12.165

Publication date:
2020

Document Version
Publisher's PDF, also known as Version of record

Available online at www.sciencedirect.com

ScienceDirect

IFAC PapersOnline CONFERENCE PAPER ARCHIVE

IFAC PapersOnLine 53-2 (2020) 13322–13327

MPPT Based Sliding Mode Control for Fuel Cell Connected Grid System

F. El Otmani * **A. Abouloifa** * **M. Aourir** * **I. Lachkar** ** **FZ. Assad** * **F. Giri** *** **JM. Guerrero** ****

* *TI Lab, FSBM, Department of Physics, Hassan II University of Casablanca, Morocco (fadwa.elotmani@gmail.com).*
** *RI Lab, ENSEM, Hassan II University of Casablanca, Morocco*
*** *Normandie UNIV, UNICAEN, ENSICAEN, LAC, 14000 Caen, France*
**** *Department of Energy Technology, 9220 Aalborg East, Denmark*

Abstract: The fuel cell has become a promising alternative to fossil sources due to its clean and efficient energy. However, it is challenging to connect the fuel cell generator to the electrical grid due to the high nonlinearity of the fuel cell. This paper deals with the problem of controlling a Proton-exchange membrane fuel cell connected to the electrical grid. In fact, a high step-up DC stage composed of an interleaved boost and a three-level boost converter, is used to ensure the maximum point power tracking, and to enhance the fuel cell voltage. Then the DC power is delivered to a half-bridge inverter and injected into the grid via an LCL filter. This study aims to design a nonlinear controller based on the sliding mode approach in order to ensure the following objectives: i) Guarantee the maximum power of the PEM Fuel cell ii) Guarantee the proper current sharing among models of IBC. iii) Regulate the interior voltage in order to improve and stabilize the FC energy. iv) Regulate the DC link voltage. v) Ensure the three-level boost series voltage balance. vi) Ensure the power factor correction. The efficiency of the proposed controller is verified and validated through numerical simulation using Matlab Simulink environment.

Keywords: Fuel cell, Three-level boost, Interleaved boost, Electrical grid, Sliding mode control, Control of renewable energy resources, Application of power electronics.

1. INTRODUCTION

Today, the widening gap between fuel production and global energy needs is causing a significant increase in fossil fuel (FF) prices. On the other hand, renewable energies such as wind, solar, and hydrogen have become promising alternatives to supply the energy market, thanks to their low cost, their abandonment, and their clean energy. Among these resources, the Proton-exchange membrane fuel cell (PEMFC) has become an attractive candidate solution due to its efficiency, low operation temperature, and fast start-up, which make it widely applied in many fields including transportation, mobile, and domestic applications Otmani et al. (2018). However, the energy generated by the FC is low compared to other energy sources and limited by the operating conditions A.Harrag and Messalti (2018). Therefore, high gain boost converters are required to interface the fuel cell systems and to improve and stabilize the PEMFC energy Han et al. (2018).

The PEMFC generator provides a DC power. Therefore, a power conditioning stage is required to connect the PEMFC to the electrical grid in order to convert the DC power into AC power. This research area has recently witnessed increased progress in research issues where many power conditionings stages (PCS) and control methods have been proposed. Indeed, Wu et al. (2017) proposed Disturbance Rejection Control of grid-connected solid-oxide fuel cell in order to improve the performance of the PCS consisting of a DC-DC converter and a DC-AC inverter. Then Sun et al. (2019) presented the fuel cell branched to double-column: the compressor and a fuel cell directly connected to the utility grid via DC/AC inverter, where an iterative algorithm developed to decouple the computational coupling and to deduce the steady-state solutions. In Reddy and Sudhakar (2018) a neural network-based maximum power point tracking (MPPT) controller for the grid-connected PEMFC system, was proposed where the Radial basis function network (RBFN) algorithm is implemented in the neural network controller to extract the maximum power from PEMFC.

This paper deals with the problem of controlling the PEMFC system connected to the electrical grid, using a PCS to manage the supplied energy. The PCS includes two major stages: i) the DC stage consists of the association of two DC boost converters (three-level boost converter (TLBC) Messikh et al. (2019) and the interleaved boost converter (IBC) Narayane and Naidu (2018)). This combination offers generally significant gain, reduced input current ripple, reduced inductor size, and switching loss Huang (2009). ii) the AC stage is a half-bridge inverter (HBI), used to match the supplied energy and to inject it into the electrical grid via an LCL filter to reduce the ripple cutting off the output current. In fact, the PEMFC has non-linear P-I characteristic due to the changes in water and oxygen flow Karami et al. (2012) that reduce

10.1016/j.ifacol.2020.12.165

the system efficiency. To overcome this limit, an MPPT block and a fuel flow regulator are employed to extract the maximum power and to ensure the good operation of the PEMFC. This study aims to design a nonlinear controller in order to achieve the following objectives: i) Guarantee the maximum power of the PEM Fuel cell ii) Guarantee the proper current sharing among models of IBC. iii) Regulate the interior voltage in order to improve and stabilize the FC energy. iv) Regulate the DC link voltage. v) Ensure the TLBC series voltage balance. vi) Ensure the power factor correction. Therefore, a nonlinear controller is designed using the sliding mode approach and based on the mathematical model of the whole system. The efficiency of the proposed controller, is supported in the Matlab Simulink environment.

The rest of the paper is organized as follows: Section 2 presents the description and the mathematical modeling of the fuel cell connected to the electrical grid system. Then, the proposed nonlinear controller based on the sliding mode approach and the MPPT algorithm, is developed in section 3 and verified in section 4 trough simulation results. Finally, conclusions are drawn, and the reference list ends the paper.

2. SYSTEM UNDERSTUDY AND PROBLEM FORMULATION

The schematic diagram shown in Fig. 1 illustrates the PEMEC connected to the electrical grid. In fact, the DC output of the FC generator is connected to a high step up stage that comprises an IBC and a TLBC convereters. The current supplied by the fuel cell travels through N distinct paths, where the number of inductors and switches is identical to the number of phases in the IBC side. Then, the DC voltage is delivered to the HBI and is injected into the electrical grid via an LCL filter.

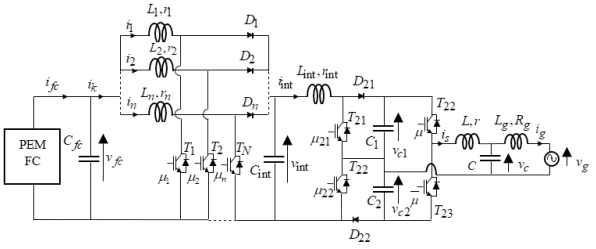

Fig. 1. Electrical circuit of the PEMFC connected grid system

Where i_{fc} and v_{fc} are respectively the current and the voltage generated by the PEMEC; $i_1 + i_2 + ... + i_n$ is the IBC input current; v_{int} is denoted the interior voltage that connects the IBC to the TLBC; i_{int} is the TLBC input current; v_{c1} and v_{c1} are denoted the DC link voltages; i_s and v_c are respectively the current in L (the input of the LCL filter) and the voltage across C ; i_g and v_g present respectively the current and the voltage of the grid; μ_1, μ_2,..., μ_n, μ_{21}, μ_{22} and μ are denoted the control inputs.

2.1 Average model

Kirchhoff laws are applied to the system illustrated in Fig. 1, where average technique is employed to obtain the below mathematical model, and the input inductances are considered identical:

$$L_g \frac{dx_1}{dt} = -R_g x_1 + x_2 - < v_g > \tag{1}$$

$$C \frac{dx_2}{dt} = x_3 - x_1 \tag{2}$$

$$L \frac{dx_3}{dt} = \frac{u}{2} w_3 + \frac{w_4}{2} - x_2 - R x_3 \tag{3}$$

$$C_{fc} \frac{dz_1}{dt} = < i_{fc} > - z_2 \tag{4}$$

$$L_k \frac{dz_2}{dt} = n z_1 - (n - u_k) w_1 - r_k z_2 \tag{5}$$

$$C_{int} \frac{dw_1}{dt} = z_2 - \sum_{j=1}^{n} u_j z_j - w_2 \tag{6}$$

$$L_{int} \frac{dw_2}{dt} = w_1 - r_{int} w_2 - w_3 + \frac{u_s}{2} w_3 - \frac{u_d}{2} w_4 \tag{7}$$

$$C_1 \frac{dw_3}{dt} = (2 - u_s) w_2 - u x_3 \tag{8}$$

$$C_2 \frac{dw_4}{dt} = u_d w_2 - x_3 \tag{9}$$

x_1, x_2, x_3, z_1, z_2, w_1, w_2, w_3, w_4, u, u_s, u_d, $u_j (j = 1, ..., n)$, and u_k denote respectively the average values over cutting periods of the signals i_g, v_g, i_s, $i_1 + i_2 + ... + i_n$, v_{int}, i_{int}, $(v_{c1} + v_{c2})$, $(v_{c1} - v_{c2})$, μ, $(\mu_{21} + \mu_{22})$, $(\mu_{22} - \mu_{21})$, and $\mu_j (j = 1, ..., n)$. Noting that this system is a high order, nonlinear system due to the products between the control signals and state variables.

3. THE SLIDING MODE CONTROLLER DESIGN

Fig. 2 shows the structure of the control strategy intended to manage the energy between the PEMFC and the electrical grid. The control strategy is developed based on the sliding mode (SM) approach and taking into account the nonlinear behavior of the FC and the power converters. In fact, the SM approach is adopted to avoid the effects of modeling uncertainties, fluctuations, and disturbance of parameter and load variations.

3.1 FC maximm power tracking

The highly nonlinear character of the PEMFC is affected by operating conditions such as temperature air, hydrogen flow rate, and pressure. As a matter of fact, one optimal operating point corresponds to the maximum power (MPP) is delivered by the PEMFC. Therefore, an MPPT algorithm based on the P&O method Madjid and Paul (2018) is employed to provide the voltage reference corresponding to the MPP in order to avoid excessive fuel consumption and low-efficiency operation. Furthermore, the FC generates a specific voltage and current for every fuel flow rate. For this reason, a hydrogen flow rate regulator

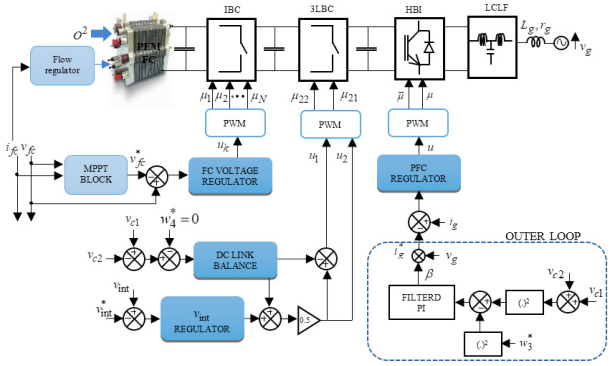

Fig. 2. Electrical circuit of the PEMFC connected grid system

is used to improve the MPPT as well as the FC efficiency Karami et al. (2012) and the fuel flow regulator can be expressed by the following equation Bizon (2014):

$$FuelFr = \frac{60000R_m(273+\theta)N_c i_{fc}}{2F(101325P_{f(H2)})(U_{f(H2)}/100)(x_{H2}/100)} \tag{10}$$

with $R_m = 8.3145J/mol$, $F = 98645As/mol$, N_c represents the number of cells in series, θ is the operating temperature, $U_{f(H2)}$ is the nominal utilization of hydrogen, $P_{f(H2)}$ is the pressure of the fuel x_{H2} is the composition of fuel.

3.2 FC regulator:

The FC regulator is developed based on the SMC to ensure the MPPT where the FC voltage must track the reference provided by the MPPT block. The first step is to define the appropriate sliding surface Otmani et al. (2017). The following equation represents the sliding surface adopted in this regulator:

$$e_{z1} = C_{fc}(z_1 - z_1^*) \tag{11}$$

where z_1^* is the voltage reference generated by the MPPT.

The sliding mode control includes two elements: i) the equivalent control u_{eq}. This law provides the main control action, then ii) the switching control u_n. This part serves to restrain the sliding mode along the sliding surface Abouloifa et al. (2018):

$$u = u_{eq} + u_n \tag{12}$$

the equivalent control law aims to maintain the SM on the selected surface while respecting the invariance condition $s = 0$. The equivalent control law is defined to be the solution of the following equation:

$$\begin{aligned}\dot{s}_{z1} =& < \dot{i}_{fc} > -\frac{1}{L_k}(nz_1 - nw_1 - r_k z_2) - \frac{1}{L_k}u_k w_1 \\ & -C_{fc}\ddot{z}_1^* + \lambda_{z1}(< i_{fc} > -z_2 - C_{fc}\dot{z}_1^*)\end{aligned} \tag{13}$$

The solution of the above equation leads to the following control law:

$$\begin{aligned}u_{keq} = \frac{1}{w_1}\{&-n(z_1 - w_1) + r_k z_2 \\ &+L_k(< \dot{i}_{fc} > -C_{fc}\ddot{z}_1^*) \\ &+L_k\lambda_{z1}(< i_{fc} > -z_2 - C_{fc}\dot{z}_1^*)\}\end{aligned} \tag{14}$$

The second part of the sliding mode control is designated to ensure global stability. Therefore the below Lyapunov function is considered:

$$v_{z1} = 0.5s_{z1}^2 \tag{15}$$

its time-derivative along the trajectory of (11) is:

$$\dot{v}_{z1} = -\frac{1}{L_k}u_k w_1 s_{z1} \tag{16}$$

the condition $s\dot{s} < 0$ must be respected to ensure the global stability. To this end, the dynamics of the Lyapunov function must be negative. Then the Lyapunov dynamics is considered as follows:

$$\dot{v}_{z1} = -s_{z1}\alpha_{z1}\tanh(\frac{s_{z1}}{\epsilon_{z1}}) \tag{17}$$

with α_{z1} and ϵ_{z1} are positive real control parameters.

The final control law is obtained by combining (14), (16), and (17)

$$u_k = u_{keq} + \frac{L_k}{w_1}\tanh(\frac{s_{z1}}{\epsilon_{z1}}) \tag{18}$$

3.3 v_{int} regulator

This regulator seeks to enhance the voltage generated by the PEMFC. The voltage w_1 must track a constant reference w_1^* higher than the value of the FC voltage. Therefore, the voltage tracking error is defined as follows:

$$e_{w1} = C_{int}(w_1 - w_1^*) \tag{19}$$

In this sense, a non-linear controller is designed based on the SMC assuming that the subsystem (4)-(5) is a second-order system $n = 2$. Then, the sliding surface is defined as follows:

$$s_{w1} = \dot{e}_{w1} + \lambda_{w1}e_{w1} \tag{20}$$

the first-time derivative of the sliding surface leads to the following equation:

$$\begin{aligned}\dot{s}_{w1} = \frac{1}{L_K}&\{nz_1 - (n-u_k)w_4 - r_k z_2\} \\ &-C_{int}(\ddot{w}_1^* + \lambda_{w1}\dot{w}_1^*) + \lambda_{w1}(z_2 - w_2) - \dot{w}_2 \\ &-\frac{d}{dt}\sum_{j=1}^{n}u_j z_j - \lambda_{w1}\sum_{j=1}^{n}u_j z_j\end{aligned} \tag{21}$$

The equivalent control law is designed by regarding the invariance condition:

$$u_{seq} = \frac{2L_{int}}{w_3}\{\frac{1}{L_k}(nz_1 - (n-u_k)w_4 - r_k z_2 + \lambda_{w1}(z_2 - w_2) - \dot{w}_2) - \frac{d}{dt}\sum_{j=1}^{n} u_j z_j - C_{int}(\ddot{w}_1^* + \lambda_{w1}\dot{w}_1^*) - \lambda_{w1}\sum_{j=1}^{n} u_j z_j\} \quad (22)$$

a Lyapunov function has the same form as (16) is considered to develop the switching control law where its dynamic is defined as follows:

$$\dot{v}_{w1} = -s_{w1}\alpha_{w1}\tanh(\frac{s_{w1}}{\epsilon_{w1}}) \quad (23)$$

with α_{w1} and ϵ_{w1} are positive real control parameters. Then, the final control law is obtained by combining (22) and (23):

$$u_s = u_{seq} + \frac{2L_{int}}{w_3}\tanh(\frac{s_{w1}}{\epsilon_{w1}}) \quad (24)$$

3.4 The DC bus voltage balance

The balance of the voltages v_{c1} and v_{c2} is necessary to ensure the smooth operation of the TLBC where the difference w_4 must follow a null reference w_4. To this end, the tracking error is represented as follows:

$$e_{w4} = C_{12}(w_4 - w_4^*) \quad (25)$$

Considering the first order subsystem (8), the deigned sliding surface and its first-time derivative are defined as follows:

$$s_{w4} = e_{w4} \quad (26)$$

$$\dot{s}_{w4} = u_d w_2 - x_3 - C_{12}\dot{w}_4^* \quad (27)$$

The equivalent control law is obtained by solving (27) and taking into account the invariance condition:

$$u_{deq} = \frac{x_3 + C_{12}\dot{w}_4^*}{w_4} \quad (28)$$

the switching law design implies the Lyapunov function and its dynamic defined as follows:

$$v_{w4} = 0.5 s_{w4}^2 \quad (29)$$

$$\dot{v}_{w4} = (u_{dn} w_2) s_{w4} \quad (30)$$

Indeed, the choice of the following dynamic of the Lyapunov function ensures the global stability respecting the convergence condition.

$$\dot{v}_{w4} = -s_{w4}\alpha_{w4}\tanh(\frac{s_{w4}}{\epsilon_{w4}}) \quad (31)$$

with α_{w4} and ϵ_{w4} are positive real control parameters.

Then, substituting (28), (30), and (31) leads to the final control law:

$$u_d = \frac{1}{w_2}(x_3 + C_{12}\dot{w}_4^* - \alpha_{w4}\tanh(\frac{s_{w4}}{\epsilon_{w4}})) \quad (32)$$

3.5 PFC Regulator

In this section, the PFC controller is a multiloop regulator that aims to ensure the power factor correction and the DC link voltage regulation. Assuming that (1)-(3) is third order subsystem. The sliding surface is defined as follows:

$$s_x = \ddot{e}_{x1} + \lambda_x^2 e_{x1} \quad (33)$$

where λ_x is a positive real control parameter and e_{x1} is the current tracking error defined as follows:

$$e_{x1} = L(x_1 - x_1^*) \quad (34)$$

To get the equivalent control law; the following sliding manifold must be solved:

$$\dot{s}_x = -\frac{R_g}{L}(-\frac{R_g}{L}\dot{x}_1 + \frac{x_3 - x_1}{C} + < \dot{v}_g >) - < \ddot{v}_g > + \frac{1}{2LC}(uw_3 + w_4) - L\dddot{x}_1^* + \frac{1}{LC}(-2x_2 - rx_3 + R_g x_1 + < v_g >) + \lambda_3^2(-R_g x_1 + x_2 - < v_g > - L\dot{x}_1^*) \quad (35)$$

Then the equivalent control law is obtained:

$$u_{eq} = \frac{2}{w_3}\{R_g C(\dot{x}_1 + \frac{x_3 - x_1}{C} - < \dot{v}_g >) - 0.5w_4 (-R_g x_1 + x_2 - < v_g >)(1 - LC\lambda_3^2) + LC(L\lambda_3^2\dot{x}_1^* + < \ddot{v}_g > + L\dddot{x}_1^*) + rx_3\} \quad (36)$$

The switching control law is defined the same way as the previous switching laws respecting the following Lyapunov function and its derivative:

$$v_x = 0.5 s_x^2 \quad (37)$$

$$\dot{v}_x = \frac{u_n}{2LC} w_3 s_x \quad (38)$$

The following dynamics is selected to ensure the convergence condition:

$$\dot{v}_x = -s_x\alpha_x\tanh(\frac{s_x}{\epsilon_x}) \quad (39)$$

with α_x and ϵ_x are positive real control parameters. The final control law is derived using (36), (38), and (39)

$$u = u_{eq} - \frac{2}{w_3}\tanh(\frac{s_x}{\epsilon_x}) \quad (40)$$

OUTER LOOP:

The outer loop aims to generate a turning signal β by means of a proportional-integral (PI) to ensure the DC link

regulation where $y_1 = w_3^2$ must pursuit the reference value $y_1^* = w_{3r}^2$. Considering the fact that β and its derivatives up to order 3 are available, the following filtered PI is considered:

$$\beta = (\frac{b}{b+s})^3(k_{y1}e_{y1} + k_{y2}e_{y2}) \tag{41}$$

With $e_{y1} = y - y^*$ and $e_{y2} = \int e_{y1}de$. s denotes the Laplace variable and (a, k_{y1}, k_{y2}) are positive real design parameters.

Theorem 1. (main result). Considering the closed-loop single-phase grid connected to a PEM fuel cell, represented by the averaged model (1)-(9) and inclosing the SMC control laws (18), (24), (32), (40), and (41). The designed regulator gives crucial results summarized as follows:

- The closed-loop system is globally asymptotically stable.
- The tracking error e_{z1} vanishes and leads to the MPPT reaching and to an equal current sharing among IBC models.
- e_{w1} also vanishes and involves the increase of the fuel cell supplied energy.
- The DC bus voltage is regulated and the balance of v_{c1} and v_{c2} is ensured when the tracking errors e_{y1} and e_{w1} converge to zero.
- The vanishment of the tracking error e_x and the convergence of the variable β to a constant, implies the PFC.

4. SIMULATION RESULTS

The simulation results aim to check the reliability of the designed control law using the MATLAB software. The PEMFC, used in the numerical simulation, is predefined by the SimPowerSystems toolbox of Matlab R2015b, where its production capacity is 8.325 kW, 37 V, and 255 A. The controller parameters, and the parameters of the system, are listed in Tables 1 and 2. The resulting closed-loop control performances are illustrated by Figs. 3-10.

Table 1. PEMFC system and signle-phase grid characteristics

Parameters	Symbols	values
interleaved boost	C_{fc}	1 mF
	$L_{k,1,2}$	8 mH
	$r_{k,1,2}$	1 $m\Omega$
Three-level Boost	C_{int}	4 mF
	L_{int}, r_{int}	0.09 mH, 2 $m\Omega$
Electrical Network	E	$220\sqrt{2}V$
	f	50 Hz
LCL-Filter	L	4 mH
	C	0.15 mF
	R, R_g	500 $m\Omega$
PWM switchingf requency	f_{pwm}	10 Khz
DC capacitance	$C_{12} = C_1 = C_2$	4 mF

Fig. 3 illustrates the PEMFC voltage follows the reference provided by the MPPT block involving the MPPT tracking, where the PEMFC current and power reach respectively 225 A and 8 kW. indeed, these values correspond to the MPP. Then, Fig. 4 exhibits the appropriate current sharing among the models of the interleaved boost. Fig. 5

Table 2. controller parametrs

Parameters	Symbols	values
Current regulator (PFC)	λ_x	$1e^9$
	α_x	$5e^{-3}$
	ϵ_x	$8e^{-3}$
Fc regulator (inner loop)	λ_{z1}	$1.5e^3$
	α_{z1}	$1e^{-1}$
	ϵ_{z1}	$8e^{-3}$
Voltage regulator (v_{int})	λ_{w1}	$1e^3$
	α_{w1}	$6e^{-2}$
	ϵ_{w1}	$5e^{-1}$
DC Link regulator	k_{y1}	$1e^{-6}$
	k_{y2}	$1e^{-5}$
	a	$15e^{-4}$
The voltage balancet	α_{w4}	$6e^{-2}$
	ϵ_{w4}	$5e^{-1}$

illustrates the achievement of the interior voltage regulation. The DC-link voltage is tightly controlled, while the balance between signals v_{c1} and v_{c2}, is ensured where their sum follow the set refrence and their difference tends to a nul value, as shown in Fig. 6. On the grid side, Fig. 7 and 8 illustrates the grid current follows its reference provided by the outer loop, and has a sinusoidal waveform in phase with the grid voltage where Fig. 9 shows the achievement of a quasi-unity power factor. Finally, Fig. 10 depicts the signal β provided by the PI regulator.

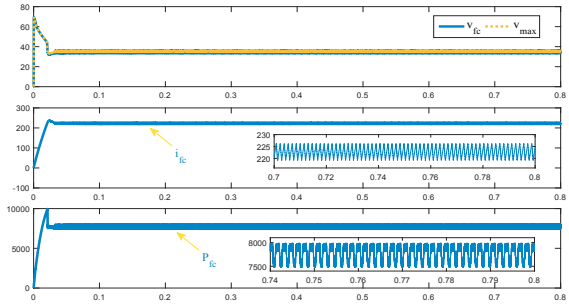

Fig. 3. PV voltage, the MPPT reference voltage, and the MPPT values of the current and the power.

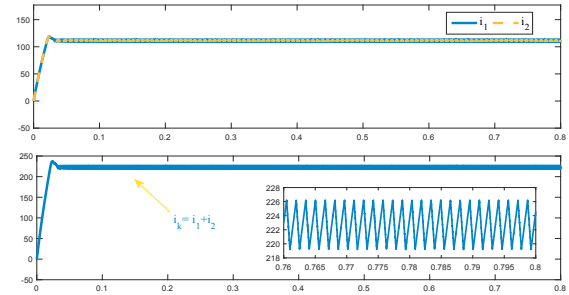

Fig. 4. the input current sharing of IBC modules

5. CONCLUSION

This work dealt with the problem of controlling a PEMFC connected to the single-phase, where nonlinear control law is elaborated based on the sliding mode approach to achieve the stated objectives. Then the proposed controller is simulated in Matlab software, where the simulation results show the efficiency of the boost stage in terms of boosting and stability and proved that the developed controller meets the control objectives.

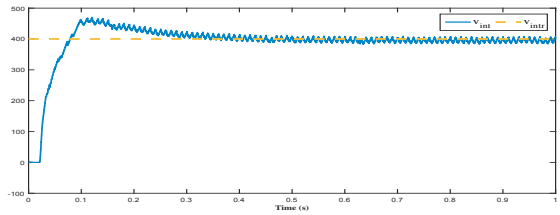

Fig. 5. interleaved boost outer voltage and its reference

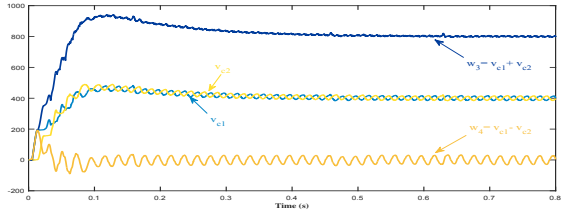

Fig. 6. DC bus voltages znd balance

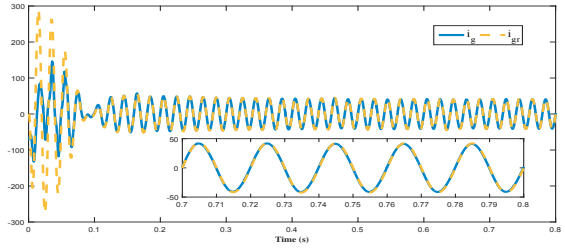

Fig. 7. Grid current waveform

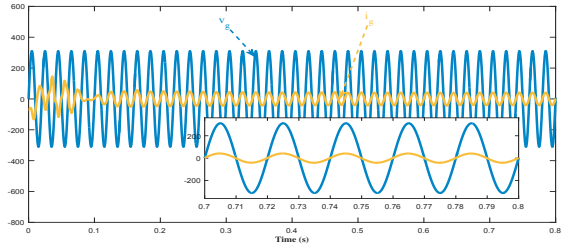

Fig. 8. Grid current and voltage

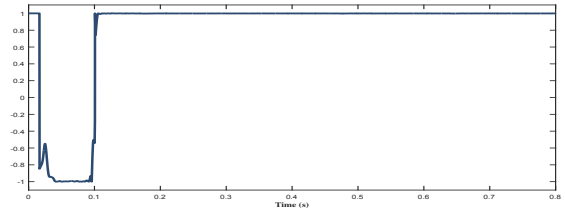

Fig. 9. Power factor

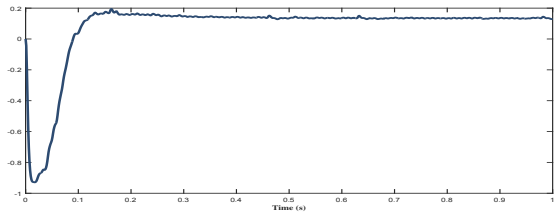

Fig. 10. External control signal β

REFERENCES

Abouloifa, A., Aouadi, C., Lachkar, I., Boussairi, Y., Aourir, M., and Hamdoun, A. (2018). Output-feedback nonlinear adaptive control strategy of the single-phase grid-connected photovoltaic system. *Journal of Solar Energy*, 2018.

A.Harrag and Messalti, S. (2018). How fuzzy logic can improve pem fuel cell mppt performances ? *International Journal of Hydrogen Energy*, 43(1), 537–550.

Bizon, N. (2014). Tracking the maximum efficiency point for the fc system based on extremum seeking scheme to control the air flow. *Applied energy*, 129, 147–157.

Han, B., Bai, C., and andd M. Kim, J.L. (2018). Repetitive controller of capacitor-less current-fed dual-half-bridge converter for grid-connected fuel cell system. *IEEE Transactions on Industrial Electronics*, 65(10), 7841–7855.

Huang, B. (2009). *Convertisseur continu-continu à rapport de transformation élevé pour applications pile à combustible*. Ph.D. thesis, Institut National Polytechnique de Lorraine.

Karami, N., Outbib, R., and Moubayed, N. (2012). Fuel flow control of a pem fuel cell with mppt. In *2012 IEEE International Symposium on Intelligent Control*, 289–294. IEEE.

Madjid, I.E. and Paul, G. (2018). Study of fuzzy logic controller based mppt and the p&o for the z-source inverter integrated in pv system. In *2018 International Conference on Electrical Sciences and Technologies in Maghreb (CISTEM)*, 1–6. IEEE.

Messikh, T., RAHIM, N., and Mekhilef, S. (2019). Sensorless second-order switching surface for a three-level boost converter. *Turkish Journal of Electrical Engineering & Computer Sciences*, 27(1), 11–23.

Narayane, P. and Naidu, H. (2018). Power factor correction (pfc) of a single phase ac to dc interleaved boost converter by using novel control scheme. *International Journal of Research*, 5(13), 498–503.

Otmani, F.E., Abouloifa, A., Aourir, M., Hamdoun, A., and Lachkar, I. (2017). Comparative study of two sliding surfaces to control a double boost converter. In *presented at the Proceedings of the International Conference on Industrial Engineering and Operations Management*, 1200–1201.

Otmani, F.E., Abouloifa, A., Aourir, M., Lachkar, I., Assad, F., and Hamdoun, A. (2018). A passivity-based control applied to a double cascade dc/dc converter using a fuel cell. In *2018 Renewable Energies, Power Systems & Green Inclusive Economy (REPS-GIE)*, 1–6. IEEE.

Reddy, K. and Sudhakar, N. (2018). A new rbfn based mppt controller for grid-connected pemfc system with high step-up three-phase ibc. *International Journal of Hydrogen Energy*, 43(37), 17835–17848.

Sun, L., Jin, Y., Pan, L., Shen, J., and Lee, K. (2019). Efficiency analysis and control of a grid-connected pem fuel cell in distributed generation. *Energy Conversion and Management*, 195, 587–596.

Wu, G., Sun, L., and Lee, K. (2017). Disturbance rejection control of a fuel cell power plant in a grid-connected system. *Control Engineering Practice*, 60, 183–192.